




## Article

# Comparison of K340 Steel Microstructure and Mechanical Properties Using Shallow and Deep Cryogenic Treatment

Patricia Jovičević-Klug<sup>1,2,\*</sup> , László Tóth<sup>3,\*</sup>  and Bojan Podgornik<sup>1,2</sup> 

<sup>1</sup> Department of Metallic Materials and Technology, Institute of Metals and Technology, Lepi pot 11, 1000 Ljubljana, Slovenia

<sup>2</sup> Jožef Stefan International Postgraduate School, Jamova c. 39, 1000 Ljubljana, Slovenia

<sup>3</sup> Bánki Donát Faculty of Mechanical and Safety Engineering, Óbuda University, Népszínház u. 8., 1081 Budapest, Hungary

\* Correspondence: patricia.jovicevicklug@imt.si (P.J.-K.); toth.laszlo@bgk.uni-obuda.hu (L.T.); Tel.: +386-1470-1990 (P.J.-K.); +36-1-66-5342 (L.T.)

**Abstract:** In this research, Böhler K340 cold work tool steel was subjected to three different heat treatment protocols, conventional heat treatment (CHT), shallow cryogenic treatment (SCT), and deep cryogenic treatment (DCT). The study compares the effect of SCT and DCT on the microstructure and consequently on the selected mechanical properties (micro- and macroscale hardness and impact toughness). The study shows no significant difference in macroscale hardness after the different heat treatments. However, the microhardness values indicate a slightly lower hardness in the case of SCT and DCT. Microstructure analysis with light (LM) and scanning electron microscopy (SEM) indicated a finer and more homogenous microstructure with smaller lath size and preferential orientation of the martensitic matrix in SCT and DCT samples compared to CHT. In addition, the uniform precipitation of more spherical and finer carbides is determined for both cryogenic treatments. Moreover, the precipitation of small dispersed secondary carbides is observed in SCT and DCT, whereas in the CHT counterparts, these carbide types were not detected. X-ray diffraction (XRD) and electron backscatter diffraction (EBSD) confirms that SCT and DCT are very effective in minimizing the amount of retained austenite down to 1.8 vol.% for SCT and even below 1 vol.% for the DCT variant.

**Keywords:** shallow cryogenic treatment (SCT); deep cryogenic treatment (DCT); cold work tool steel; microstructure; mechanical properties



**Citation:** Jovičević-Klug, P.; Tóth, L.; Podgornik, B. Comparison of K340 Steel Microstructure and Mechanical Properties Using Shallow and Deep Cryogenic Treatment. *Coatings* **2022**, *12*, 1296. <https://doi.org/10.3390/coatings12091296>

Academic Editor: Diego Martinez-Martinez

Received: 20 July 2022

Accepted: 31 August 2022

Published: 2 September 2022

**Publisher's Note:** MDPI stays neutral with regard to jurisdictional claims in published maps and institutional affiliations.



**Copyright:** © 2022 by the authors. Licensee MDPI, Basel, Switzerland. This article is an open access article distributed under the terms and conditions of the Creative Commons Attribution (CC BY) license (<https://creativecommons.org/licenses/by/4.0/>).

## 1. Introduction

Cold work tool steels are used for producing tools for cutting and forming processes such as punching, blanking, cold rolling, extruding, deep drawing, bending, and pressing. Therefore, these steels need high hardness, high abrasive and adhesive wear resistance, high compressive strength, high toughness, and improved dimensional stability [1]. One of these steels is also Böhler K340 cold work tool steel, which has a higher Cr (around 8 wt.%) and C (around 1.1%) alloying content and is produced through electroslag remelting (ESR) [2–4]. The ESR technology is mainly used to reduce inhomogeneity, such as segregations and shrink voids, and to improve the cleanness level, especially in regard to larger non-metallic inclusions [1].

Due to its unique chemical composition and properties, Böhler K340 has been highly demanded in the industry for high-performance applications [2,5]. However, in order to achieve these favorable properties also, the applied heat treatment needs to be well defined and optimized. The most commonly used heat treatment in the tool industry is conventional heat treatment (CHT), which consists of slow heating to the hardening temperature, holding at that temperature for a certain amount of time to obtain homogenous austenite grains and tailor their size to adapt the final steel properties. This part of the process can be considerably segmented into different steps, i.e., preheating, during which the heated steel

is held at intermediate temperatures to thermally equalize the surface and the core. After the hardening process, the material is quenched (rapidly cooled) at high cooling rates to temperatures below 100 °C and finally double or triple tempered at a lower temperature than the hardening temperature [1]. As a result, the microstructure of such steels normally consists of tempered martensite, retained austenite (RA), and precipitated carbides (MxC and MxCy) [5].

Another option is also to expose the material to cryogenic temperatures performed within the heat treatment path. During cryogenic treatment/technology (CT), steel is exposed to subzero temperatures in order to come close to the martensite finish temperature ( $M_f$ ). This enables us to obtain the highest possible martensite fraction in the steel in order to gain the preferable higher hardness and strength properties [6–8]. However, this may cause micro-cracking and cracking of the steel if it is not followed by a tempering step [9,10]. Nevertheless, cold work tool steels are generally triple tempered at higher tempering temperatures without CT [2,11–14], which normally results in a low RA content and sufficient dimensional stability [15]. Part of CT is also shallow cryogenic treatment (SCT) (temperature to  $-160$  °C) and deep cryogenic treatment (DCT) (temperatures below  $-160$  °C) [16]. Both treatments are an effective method to reduce the amount of RA [14,17] in order to improve materials properties and, with it, increase the tool service life [18]. As such, CT can improve the mechanical properties (hardness, impact toughness) [8,17], resulting from the highest martensite fraction as well as due to the increased precipitation and formation of very small carbides between or within the tempered martensitic grains [12,19,20]. The newly formed carbides reduce the internal stress of the martensite and also act as buffers for the microcrack propagations [21]. SCT and DCT can both induce precipitation of finer and more spherical carbides [22], resulting in a more homogenous microstructure [22,23]. However, SCT and DCT have, in the end, different levels of effect on the microstructure due to the different cooling temperatures and, with it, different effects on the final properties [7].

The aim of this research study was to compare the effect of shallow (SCT) and deep cryogenic treatments (DCT) to conventional heat treatment (CHT) in terms of changes induced in microstructure and selected mechanical properties (hardness, microhardness, and impact toughness) of cold work tool steel K340. The study also aims to provide new insight into basic research of rival cryogenic treatments.

## 2. Materials and Methods

### 2.1. Material and Heat Treatment

The selected experimental material was Böhler K340 Isodur cold work tool steel produced by electroslag remelting (ESR) technology. The samples were cut from a rectangular raw bar with charmless wire electrical discharge machining (WEDM) using Fi 240 S2P machine from GF Machines and Technologies, Biel, Switzerland. Material was cut into small pieces of  $55 \times 10 \times 10$  mm that were afterward fine-ground and polished. The chemical composition of steel was analyzed with a Hitachi PMP2 type instrument (Hitachi, Udem, Germany). The given chemical composition in wt.% is: 1.12% C, 0.92% Si, 0.39% Mn, 8.25% Cr, 2.19% Mo, 0.27% Ni, 0.15% Nb, 0.40% V, 0.14% W, and Fe as base.

Specimens were processed using three different heat treatments: the first was conventional heat treatment (CHT), the second was heat treatment involving subzero cooling after quenching to  $-150$  °C (123 K), referred to as shallow cryogenic temperature or treatment (SCT), and the third heat treatment involving deep cryogenic treatment (DCT), where the samples were cooled down to  $-196$  °C (77 K).

The selected heat treatment for each group is provided in Figure 1. All samples were first austenitized and quenched in a single step, either in a horizontal vacuum furnace IPSEN VTTC-324R, Ipsen, Kleve, Germany (DCT) or in a vacuum furnace IVA Schemetz IU72, Menden, Germany (CHT and SCT), with uniform high-pressure gas quenching using  $N_2$  at the pressure of 8 bars (average quenching rate was approximately  $7\text{--}8$  °C  $s^{-1}$ ). After quenching, the CHT group went directly for triple tempering at an aver-

age temperature of 555 °C for 2 h, whereas SCT and DCT groups went first for cryogenic treatment (CT) and then followed by triple or single tempering under the same conditions (555 °C/2 h), Figure 1. The second group was subjected to SCT, performed immediately after quenching by cooling the specimens in the IVA Schmetz IU72 vacuum furnace, using the cool plus cryogenic process in liquid nitrogen at −150 °C for 50 min, and finalized by triple tempering. The third group, DCT, was gradually immersed in liquid nitrogen for 24 h (1 day) at −196 °C after quenching, followed by only a single tempering cycle, which is reported to be adequate enough to provide the nearly complete RA transformation into martensite, when combined with DCT [24].

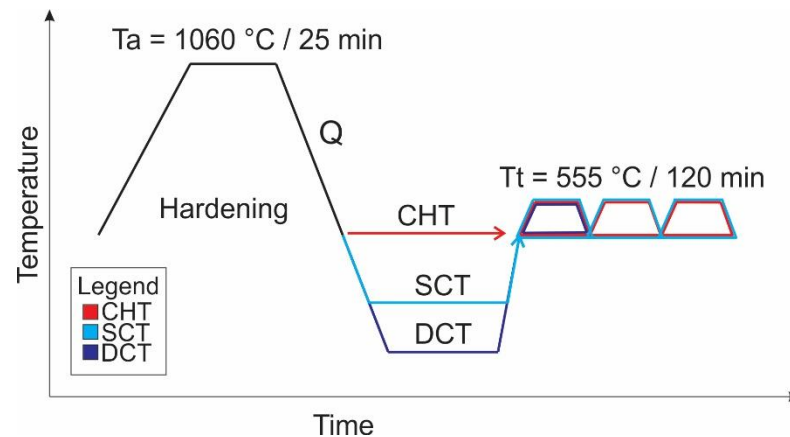


**Figure 1.** Scheme of all three heat treatments (CHT = conventional heat treatment, SCT = shallow cryogenic treatment and DCT = deep cryogenic treatment) with selected heat treatment temperature ( $T_a$  = austenitization temperature and time and  $T_t$  = tempering temperature and time).

## 2.2. Methods

### 2.2.1. Mechanical Testing

The effectiveness of the heat treatments was checked by evaluating three mechanical properties: hardness, microhardness, and impact toughness. Hardness was measured by Rockwell C hardness measurement with Instron B2000, Instron; Norwood, MA, USA, according to SIST EN ISO 6508-1:2016 standard. Microhardness was measured with Instron Tukon 2100B, Instron, Norwood, MA, USA, according to standard SIST EN ISO 6507-1:2016. For both hardness measurements, 10 samples were measured. For impact testing, a Charpy impact test machine of type RM 201 by VEB WPM, Leipzig, Germany, was used and performed on 10 samples.

### 2.2.2. Microstructure and Phase Analysis

Basic microstructural analysis was performed on polished and etched (etched by Nital for a few seconds, depending on each sample [25]) samples by ZEISS Axio Imager, Carl Zeiss, Oberkochen, Germany. Detailed microstructure characterization was performed with SEM, SM-6500 F, Jeol, Tokyo, Japan, where secondary electrons (SE), backscattered electrons (BSE), energy dispersive X-ray spectroscopy (EDX) with 15 keV electron beam Oxford EDX INCA Energy 450, detector type INCA X-SIGHT LN<sub>2</sub>, Oxford Instruments, UK and electron backscatter diffraction (EBSD) with 15 keV electron beam and current of around 5 nA were used. For EBSD data analysis, OIM Analysis software, EDAX, Ametek Inc., Warrendale, PA, USA was employed. Phase and phase fraction determination of samples via X-ray diffraction (XRD) was carried out on PANalytical 3040/60, Almelo, The Netherlands. The phase identification analysis and interpretation were performed using COD database references, and their fractions were evaluated using a combination of Rietveld refinement and Toraya method [26]. The standard evaluation error for each phase was determined to be 1–2 vol.%.



### 3. Results

#### 3.1. Microstructure and Phase Analysis

Microstructural analysis was first conducted with light (optical) microscopy in order to obtain an overview of the final microstructure of all three heat treatments, CHT, SCT, and DCT (Figure 2a–c).

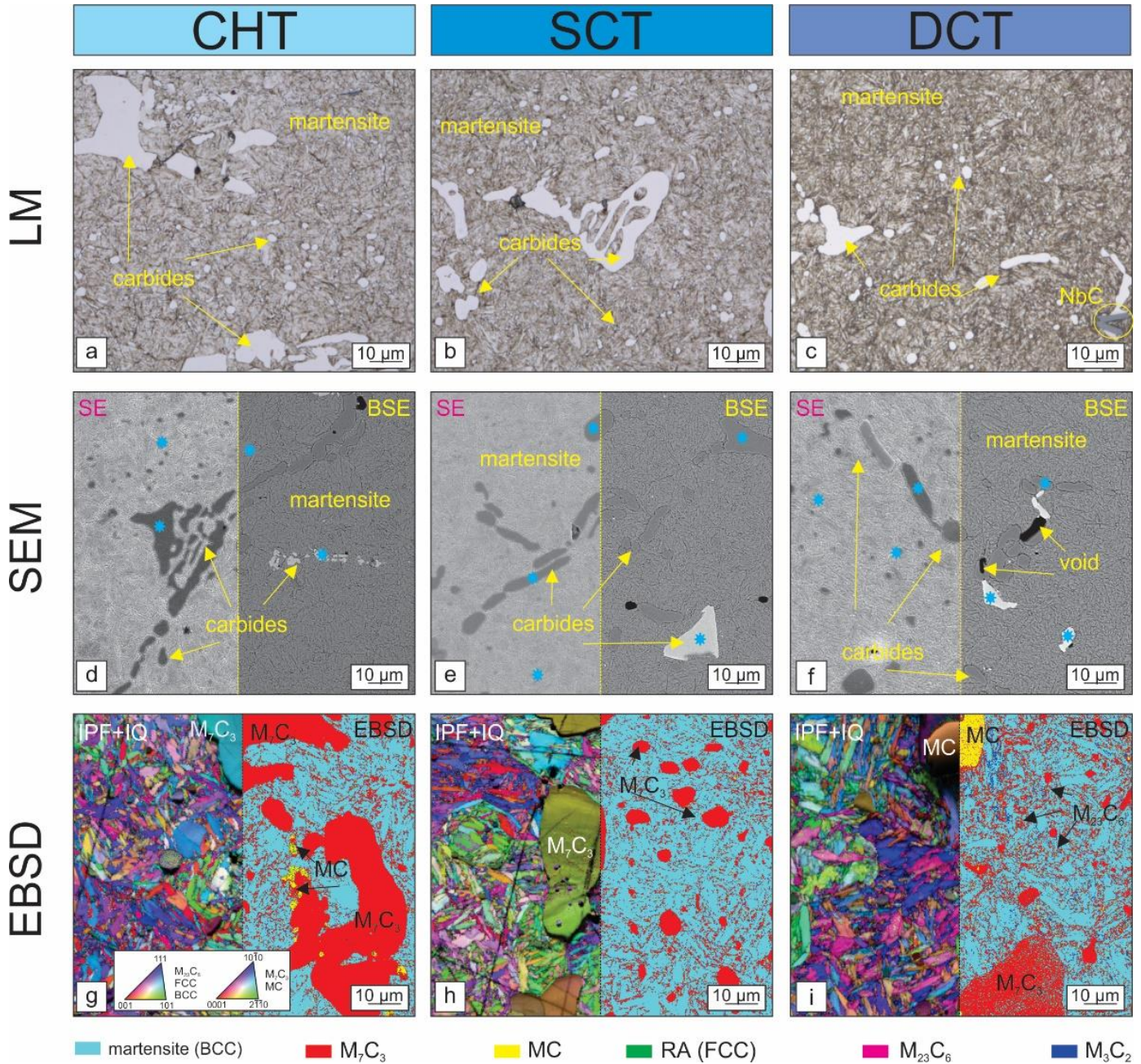


**Figure 2.** The microstructure of all three heat treatment groups CHT-conventional heat treatment (a,d,g), SCT-shallow cryogenic treatment (b,e,h) and DCT-deep cryogenic treatment (c,f,i) observed with light microscopy (LM), scanning electron microscopy (SEM) under secondary electrons (SE) and backscatter electrons (BSE) and with electron backscatter diffraction (EBSD) represented through inverse pole figures (IPF+IQ). The phases, which are presented are martensite (BCC), retained austenite (RA) and different carbides (MC,  $M_7C_3$ ,  $M_{23}C_6$  and  $M_3C_2$ ).

In-detail analysis of the microstructure, such as type, size, number, volume fraction, and distribution of phases conducted by SEM, EDS, and EBSD, is presented in

Figures 2, 3 and 4a and by XRD in Figure 4b. For all three groups, the matrix consists of lath martensite with some amount of RA (see Table 1). On average, the martensitic laths were finer with each cryogenic treatment by 21% and 33% with SCT and DCT, respectively (Figures 2a–f and 3). Accordingly, the size of martensitic laths is roughly 22% smaller with DCT compared to SCT. The martensitic laths of both SCT and DCT samples also display an overall preferential orientation along [101] and [001] directions compared to the laths of the CHT sample. Furthermore, in DCT samples, the martensitic laths displayed even more distinctively set orientation towards the [101] and [001] directions compared to the laths of the SCT sample (Figure 2g–i).

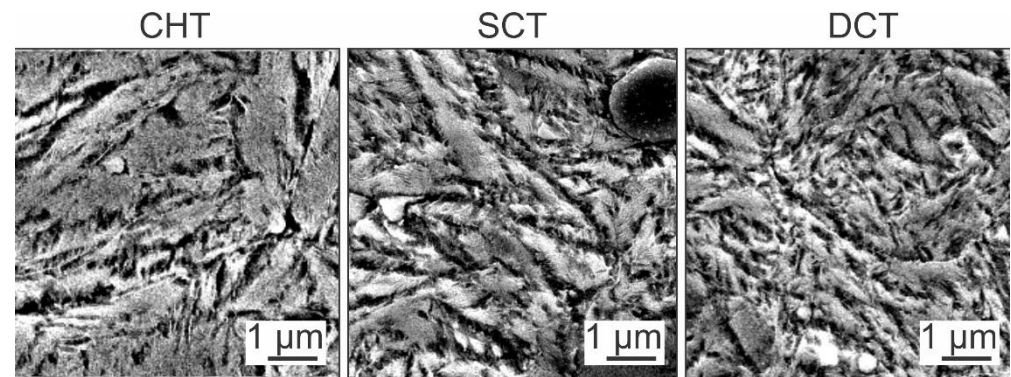


**Figure 3.** Enlarged SEM micrographs of the etched martensitic matrix presenting the martensitic lath refinement with shallow cryogenic treatment (SCT) and deep cryogenic treatment (DCT) compared to conventional heat treatment (CHT).

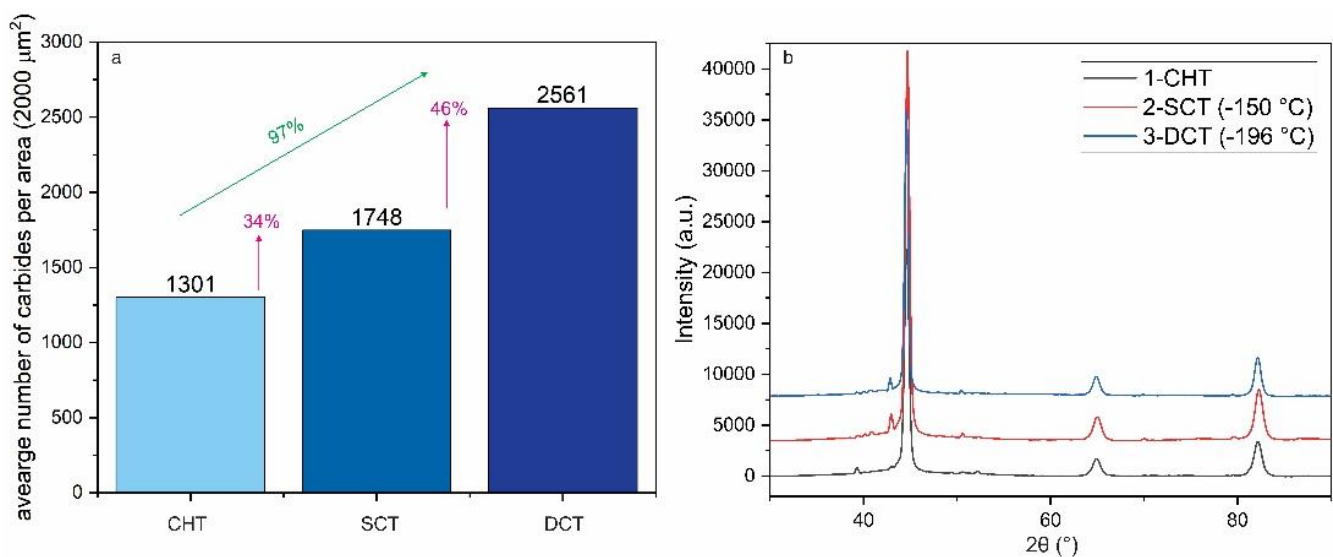


**Figure 4.** (a) the graph represents the average number of carbides per area ( $2000 \mu\text{m}^2$ ), where at least 5 locations were measured per sample. (b) X-ray diffraction (XRD) of CHT (black line), SCT (red line) and DCT (blue line) samples.

In regards to the precipitated carbides, the majority of them are formed in-between martensitic laths. The analysis of the number of precipitated carbides revealed that both SCT and DCT increased the precipitation of carbides by 34% and 97%, respectively (Figure 4a), equating to a 46% increase in precipitation with DCT compared to SCT. Furthermore, the SCT and DCT have been shown to influence the shape and average size of the carbides, at which more spherical-shaped carbides are present, with a reduced chance of agglomerations for the cryogenic variants compared to the CHT samples. Carbides distribution and size analysis, determined with EBSD, also reveals that SCT and DCT promote precipitation of



finer carbides ( $\leq 0.5 \mu\text{m}$ ) and induce a more homogenous microstructure compared to CHT counterparts, especially DCT (Figure 2d–f).

**Table 1.** Mean volumetric fractions of phases present in the samples; CHT—conventionally heat-treated; SCT—shallow cryogenically heat-treated; DCT—deep cryogenically heat-treated.

Phase (vol.%)	Heat Treatment		
	CHT	SCT ( $-150 \text{ }^\circ\text{C}$ )	DCT ( $-196 \text{ }^\circ\text{C}$ )
Martensite	53.0	55.0	50.5
RA	6.2	1.8	0.9
MC (V, Nb)	5.2	4.8	4.9
$\text{M}_7\text{C}_3$ (Cr, Fe)	16.7	24.6	28.3
$\text{M}_{23}\text{C}_6$ (Cr, Fe)	5.8	6.1	8.1
$\text{M}_3\text{C}_2$ (Cr, Fe)	13.1	7.7	7.3

XRD data (Figure 4b, Table 1) confirm that the matrix of all three samples consists mainly of martensite, with the highest vol.% for SCT (55.0). In all three groups, RA is still present. However, the presence of RA is strongly decreased by both cryogenic treatments, from 6.2 vol.% in CHT to 1.8 vol.% by SCT (reduction by 71%) and even below 1 vol.% by DCT (reduction higher than 85%), being below the detection limit. In all three heat treatment groups, the presence of  $\text{M}_2\text{C}$ ,  $\text{M}_7\text{C}_3$ ,  $\text{M}_3\text{C}_2$  and  $\text{M}_{23}\text{C}_6$  carbides is determined.

The crystal structure and chemical composition of carbides are determined with a combination of XRD and EBSD (Figures 2g–i and 4b and Table 1) and EDS (Figure 2d–f, blue marking where the analysis was performed) and EDS mapping (Figure 5). Carbides MC are shown to be enriched by V and Nb,  $\text{M}_7\text{C}_6$ ,  $\text{M}_{23}\text{C}_6$ , and  $\text{M}_3\text{C}_2$  with Cr and Fe. Further analysis showed the difference in carbide precipitation between SCT and DCT compared to CHT. The greatest difference is observed in relation to  $\text{M}_7\text{C}_3$  precipitation, where SCT precipitation is increased by roughly 50% and with DCT by around 70%, compared to the CHT group. The  $\text{M}_{23}\text{C}_6$  carbide group is predominant in the DCT group (8.1 vol.%), whereas in SCT (6.1 vol.%) and in CHT (5.8 vol.%), the values are similar. DCT also yields an increase in  $\text{M}_{23}\text{C}_6$  precipitation compared to the other two groups by approximately 35%. The general tendency of  $\text{M}_3\text{C}_2$  reflects a decrease in their formation for both CTs, equating to a 40% decrease.

### 3.2. Mechanical Properties

#### 3.2.1. Hardness and Microhardness

The results of hardness measurements (Figure 6a) show a slight decrease of less than 5% in hardness from CHT to SCT/DCT and from 60 HRC to 59 HRC. For both cryogenic treatments, the values of hardness are the same. However, for the microhardness (Figure 6b), values drop from 810 HV 0.1 for CHT to about 760 HV 0.1 for SCT and DCT (around 7% decrease compared to CHT).

#### 3.2.2. Impact Toughness

Impact toughness results presented in energy required to break CVN samples of tested cold work tool steel Böhler K340 Isodur (Figure 6c) show significant improvement for both cryogenic treatments. Impact toughness increased from 4 J for CHT to 8.5 J for SCT (increase by roughly 113%) and 8 J for DCT (increase by 100%), accordingly. Considering measurement uncertainty and scatter, both cryogenic treatments show similar results. These results are also complementary to the results of decreased hardness after both cryogenic treatments, SCT and DCT, accordingly.

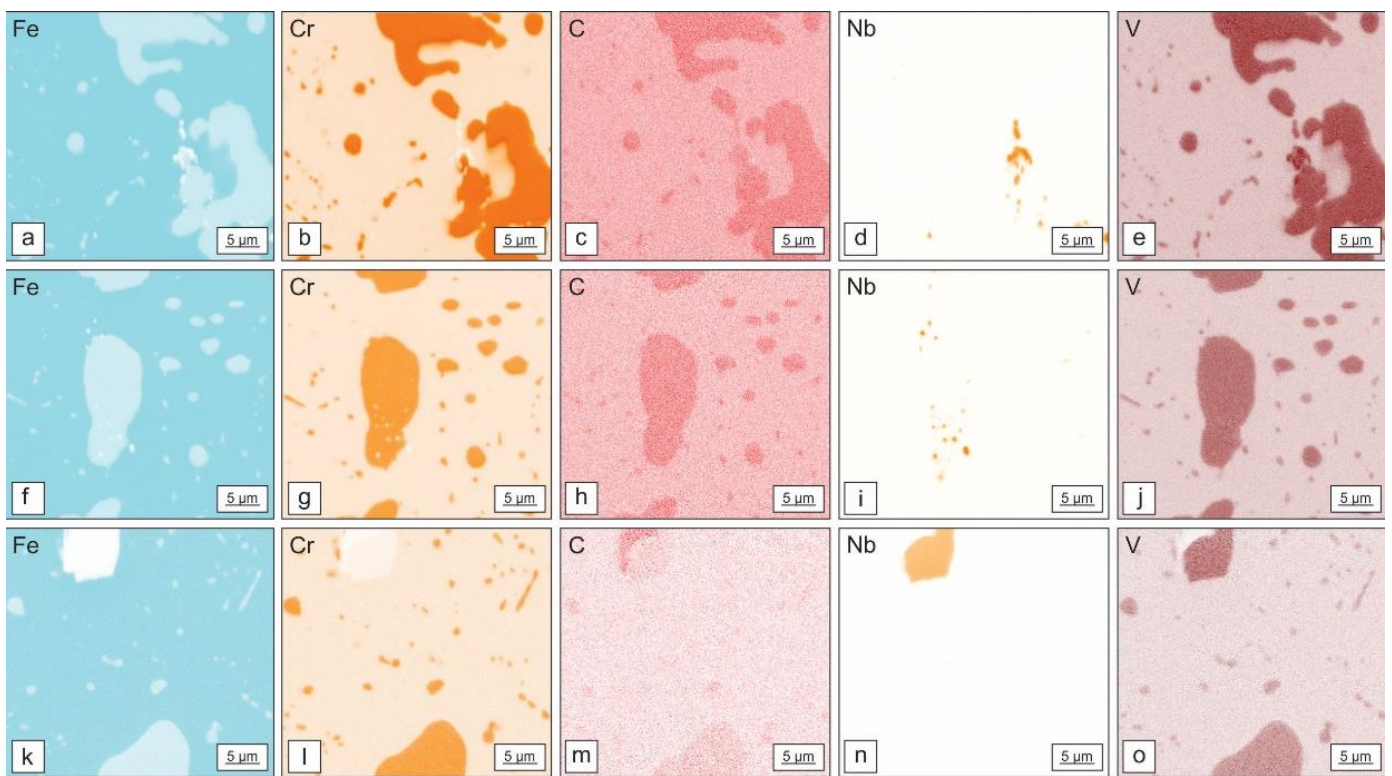


**Figure 5.** EDS-mapping of all three samples: CHT (a–e), SCT (f–j) and DCT (k–o) for Fe, Cr, C, Nb and V.

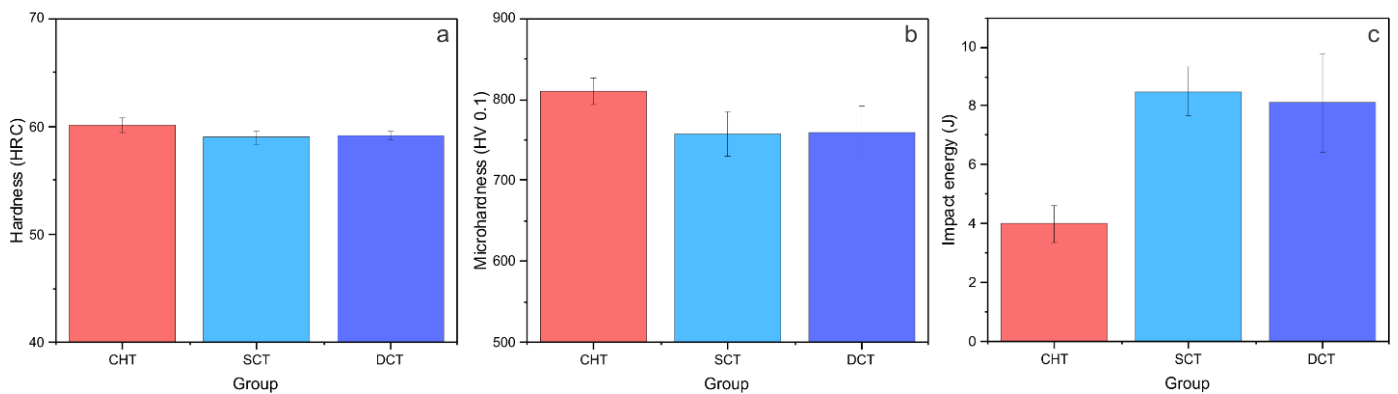


**Figure 6.** Tested mechanical properties: (a) hardness in HRC, (b) microhardness in HV 0.1 and (c) impact toughness in J.

## 4. Discussion

### 4.1. Influence of Different Cryogenic Treatments on Microstructure

Microstructural changes were strongly linked to the selected heat treatment. Both samples, SCT and DCT, after tempering, show a reduced amount of RA compared to the CHT sample, which confirms that CT reduces the amount of RA [27,28]. Furthermore, with DCT, additional conversion of RA into martensite by roughly 50% compared to SCT is achieved due to the lower treatment temperature ( $-196\text{ }^{\circ}\text{C}$ ). Additionally, the CTs also modified the martensitic matrix, which was more refined and preferably oriented along [101] and [001], which was also observed by Jovičević-Klug et al. 2021 [29] for a different type of cold work tool steel and other steels. The reasoning for such a change is related to the preferential formation of martensite laths from austenite during direct non-diffusional conversion under cryogenic temperature (case of SCT and DCT) rather than through the decomposition of RA with tempering (case of CHT). As a result, the martensitic laths for the

SCT case do show a slightly lower orientational preference compared to the DCT sample due to the small amount of RA not transformed during SCT that still partially decomposes during the subsequent tempering stage.

The observation of carbide precipitation showed that both SCT and DCT induce precipitation of carbides. In this study, the precipitation of the  $M_{23}C_6$  carbide group is the highest for the DCT group. However, for SCT, no significant difference compared to CHT was determined. The reason for induced overall carbide precipitation in the DCT group is due to the very low temperature, which causes carbon redistribution that influences the carbide formation during the later tempering stage [30]. For the DCT group also, the highest amount of  $M_7C_3$  carbide group precipitation was observed, which could be linked to the suppression of the precipitation of the stable  $M_3C_2$  during tempering, which was also confirmed by Jurči et al. 2021 for another cold work tool steel [31]. Furthermore, this dynamic can also be linked to the C and Cr content and their distribution in the matrix, as observed by Jovičević-Klug et al. 2021 [23]. The additional observation of the precipitated carbide groups also shows that both SCT and DCT groups have equally lower  $M_3C_2$  carbides compared to CHT. The possible explanation is that already cryogenic temperature below  $-150\text{ }^\circ\text{C}$  (both SCT and DCT) induces the precipitation of transition carbides [31] that effectively modify the carbide evolution pathway during tempering.

#### 4.2. Hardness and Microhardness

In selected cold work tool steel Böhler K340 Isodur a decrease in hardness and microhardness after application of cryogenic treatment (SCT and DCT) was observed.

The decrease in (micro)hardness after the application of cryogenic treatment can be correlated to the decrease in carbon content in the martensitic matrix after SCT/DCT, which then leads to reduced solid solution strengthening. A similar effect was observed by Li et al. 2018 [32] and Jovičević-Klug et al. 2021 for other steels [21]. In addition, both SCT and DCT alter the carbide precipitation, as the RA decomposition does not occur during tempering in contrast to the CHT group. Subsequently, this causes an increase in the number and density of homogeneously distributed carbides (see Section 3.1. Microstructure and phase analysis), but with finer sizes. For this reason, the matrix has a dominant effect during the indentation measurement. The overall drop in the hardness of the CTs compared to CHT can also be related to the change in the carbide precipitation that increases the occurrence of  $M_7C_3$  compared to  $M_3C_2$ . As the  $M_3C_2$  are generally harder compared to the  $M_7C_3$ , the hardness and microhardness should also generally drop for both CTs.

#### 4.3. Impact Toughness

The changes in impact toughness of different heat treatments are strongly linked to the matrix and its cohesion. The increase in impact toughness for both cryogenic treatments (SCT and DCT) is correlated to the finer martensitic laths compared to the CHT group. The increase in impact toughness can also be correlated to a more homogeneous distribution of the carbides and the cohesion between carbides and matrix. In both SCT and DCT, the additional increased  $M_7C_3$  carbide precipitation was present compared to CHT. As a result, these carbides form a more spherically-shaped form that reduces the tearing of the matrix due to reduced local stress concentration that normally forms due to oblique-shaped edges of other nano-sized carbides, such as  $M_3C_2$ . Moreover, the slight change in the impact energy for SCT can be explained by the higher presence of RA compared to DCT. In spite of the higher RA in CHT, the presence of  $M_3C_2$  carbides effectively reduce the impact energy due to their higher brittleness and lower cohesion with the matrix. Furthermore, the increase in impact energy after SCT and DCT can be correlated to the decrease in carbon presence in the martensitic solid solution during cryogenic treatment, which increases the toughness of the martensitic matrix. A similar observation was also observed in high-alloyed steels by Li et al. 2016 [33,34].



#### 4.4. Comparison of SCT vs. DCT

When comparing SCT and DCT cryogenic treatments, some distinctive differences can be observed favoring one or another type. The more effective treatment for minimizing the amount of RA within the matrix is DCT, where the RA vol.% is below 1%. In DCT also, finer martensitic laths and increased  $M_{23}C_6$  precipitation are present compared to the SCT, which may favor an increase in (micro)hardness for specific heat treatment parameters (austenitizing, tempering). In both treatments, the increase in carbide precipitation is observed with a more homogenous distribution.

However, there are some important changes in the precipitated types of carbides. In both SCT and DCT, the transient carbide type  $M_3C_2$  is reduced, which additionally influences the overall toughness of the steel. All these differences add up to the change in mechanical properties. As a result, the usage of the different CTs depends on the targeted properties. For an increase in hardness of the material, DCT might be preferable, whereas, for an increase in toughness, SCT would be preferable for cold work tool steel Böhler K340 Isodur.

### 5. Conclusions

The study investigated the influence of different cryogenic treatments, shallow (SCT) and deep cryogenic treatment (DCT), on cold work tool steel Böhler K340 Isodur in correlation to changes in microstructure and mechanical properties, namely hardness and impact toughness. The following conclusions have been established:

- I. SCT and DCT are effective methods in lowering RA presence within the matrix by 71% and 82%, accordingly. SCT and DCT groups have finer martensitic laths, which are oriented along [101] and [001]. The martensitic laths are finer by 21% and 33% with SCT and DCT, respectively.
- II. SCT and DCT influence the carbide precipitation of  $M_{23}C_6$  (5% by SCT and 35% by DCT) and  $M_7C_3$  (50% by SCT and 70% by DCT) carbide groups and also reduce the formation of transient carbide group ( $M_3C_2$ ), which is directly linked to the cryogenic temperatures.
- III. Hardness and microhardness were not significantly influenced (increase by roughly 5% for both groups) by SCT and DCT and are thus considered to not be a consistent indicator for comparing cryogenic treatments in relation to the microstructural changes.
- IV. Impact toughness was increased by both cryogenic treatments by more than 100% (by SCT 113% and by DCT 100%).
- V. For an increase in hardness of the cold work tool steel Böhler K340 Isodur, DCT is recommended, whereas, for an increase in toughness, SCT is preferable.

**Author Contributions:** Conceptualization, P.J.-K., L.T. and B.P.; methodology, P.J.-K., L.T. and B.P.; validation, P.J.-K., L.T. and B.P.; investigation, P.J.-K., L.T. and B.P.; resources, L.T. and B.P.; writing—original draft preparation, P.J.-K., L.T. and B.P.; visualization, P.J.-K.; writing-and editing P.J.-K., L.T. and B.P., supervision, P.J.-K., L.T. and B.P. All authors have read and agreed to the published version of the manuscript.

**Funding:** This research was funded by Slovenian Research Agency (ARRS), grant number P2-0050.

**Institutional Review Board Statement:** Not applicable.

**Informed Consent Statement:** Not applicable.

**Data Availability Statement:** Not applicable.

**Acknowledgments:** Authors would like to thank vacuum-heat treatment, mechanical and metallographic labs at IMT, Barbara Šetina Batič for the help with XRD measurements and for fruitful discussion and help with data to Matic Jovičević-Klug.

**Conflicts of Interest:** The authors declare no conflict of interest.

## References

1. Totten, G.E. *Steel Heat Treatment Handbook*, 2nd ed.; CRC Press: Boca Raton, FL, USA, 2007.
2. Tóth, L.; Réka, F. The Effects of Quenching and Tempering Treatment on the Hardness and Microstructures of a Cold Work Steel. *Int. J. Eng. Manag. Sci.* **2019**, *4*, 286–294. [[CrossRef](#)]
3. Toth, L. Cryogenic Treatment against Retained Austenite. In Proceedings of the Mérnöki Szimpózium a Bánkiban, Budapest, Hungary, 18 November 2021; pp. 181–186.
4. Chumanov, I.V.; Chumanov, V.I. Technology for Electroslag Remelting with Rotation of the Consumable Electrode. *Metallurgist* **2001**, *45*, 125–128. [[CrossRef](#)]
5. Zamborsky, D.S. Control of Distortion in Tool Steels. In *The Heat Treating Source Book*; ASM International: Materials Park, OH, USA, 1998; pp. 73–79.
6. Baldissera, P.; Delprete, C. Deep Cryogenic Treatment: A Bibliographic Review. *Open Mech. Eng. J.* **2008**, *2*, 1–11. [[CrossRef](#)]
7. Senthilkumar, D. Cryogenic Treatment: Shallow and Deep. In *Encyclopedia of Iron, Steel, and Their Alloys*; Totten, G.E., Colas, R., Eds.; Taylor and Francis: New York, NY, USA, 2016; pp. 995–1007. ISBN 9781351254496.
8. Pellizzari, M.; Molinari, A. Deep Cryogenic Treatment of Cold Work Tool Steel. In Proceedings of the 6th International Tooling Conference, Stockholm, Sweden, 10–13 September 2002; pp. 657–669.
9. Kalsi, N.S.; Sehgal, R.; Sharma, V.S. Cryogenic Treatment of Tool Materials: A Review. *Mater. Manuf. Processes* **2010**, *25*, 1077–1100. [[CrossRef](#)]
10. Sonar, T.; Lomte, S.; Gogte, C. Cryogenic Treatment of Metal—A Review. In *Materials Today: Proceedings*; Elsevier: Amsterdam, The Netherlands, 2018; Volume 5, pp. 25219–25228.
11. Amini, K.; Nategh, S.; Shafyei, A. Influence of Different Cryotreatments on Tribological Behavior of 80CrMo12 5 Cold Work Tool Steel. *Mater. Des.* **2010**, *31*, 4666–4675. [[CrossRef](#)]
12. Podgornik, B.; Uršič, D.; Paulin, I. Effectiveness of Deep Cryogenic Treatment in Improving Mechanical and Wear Properties of Cold Work Tool Steels. *Int. J. Microstruct. Mater. Prop.* **2017**, *12*, 216. [[CrossRef](#)]
13. Li, J.; Cai, X.; Wang, Y.; Wu, X. Multiscale Analysis of the Microstructure and Stress Evolution in Cold Work Die Steel during Deep Cryogenic Treatment. *Materials* **2018**, *11*, 2122. [[CrossRef](#)]
14. Kus, M.; Jurci, P.; Durica, J. Microstructure and Hardness of Cold Work Vanadis 6 Steel after Subzero Treatment at  $-140\text{ }^{\circ}\text{C}$ . *Adv. Mater. Sci. Eng.* **2018**, *2018*, 1–7.
15. Su, Y.Y.; Chiu, L.H.; Chen, F.S.; Lin, S.C.; Pan, Y.T. Residual Stresses and Dimensional Changes Related to the Lattice Parameter Changes of Heat-Treated JIS SKD 11 Tool Steels. *Mater. Trans.* **2014**, *55*, 831–837. [[CrossRef](#)]
16. Jovičević-Klug, P.; Podgornik, B. Review on the Effect of Deep Cryogenic Treatment of Metallic Materials in Automotive Applications. *Metals* **2020**, *10*, 434. [[CrossRef](#)]
17. Jurči, P.; Ptačinová, J.; Sahul, M.; Dománková, M.; Dlouhy, I. Metallurgical Principles of Microstructure Formation in Sub-Zero Treated Cold-Work Tool Steels—a Review. *Matériaux Tech.* **2018**, *106*, 104–113. [[CrossRef](#)]
18. Zhou, Z.C.; Du, J.; Yan, Y.J.; Shen, C.L. The Recent Development of Study on H13 Hot-Work Die Steel. *Solid State Phenom.* **2018**, *279*, 55–59. [[CrossRef](#)]
19. Villa, M.; Somers, M.A.J. Cryogenic Treatment of Steel: From Concept to Metallurgical Understanding. In Proceedings of the 24th International Federation for Heat Treatment and Surface Engineering Congress, Nice, France, 26–29 June 2017.
20. Min, N.; Li, H.M.; Xie, C.; Wu, X.C. Experimental Investigation of Segregation of Carbon Atoms Due to Sub-Zero Cryogenic Treatment in Cold Work Tool Steel by Mechanical Spectroscopy and Atom Probe Tomography. *Arch. Metall. Mater.* **2015**, *60*, 1110–1113. [[CrossRef](#)]
21. Jovičević-Klug, P.; Puš, G.; Jovičević-Klug, M.; Žužek, B.; Podgornik, B. Influence of Heat Treatment Parameters on Effectiveness of Deep Cryogenic Treatment on Properties of High-Speed Steels. *Mater. Sci. Eng. A* **2022**, *829*, 142157. [[CrossRef](#)]
22. Jovičević-Klug, P.; Jovičević-Klug, M.; Podgornik, B. Effectiveness of Deep Cryogenic Treatment on Carbide Precipitation. *J. Mater. Res. Technol.* **2020**, *9*, 13014–13026. [[CrossRef](#)]
23. Jovičević-Klug, P.; Jovičević-Klug, M.; Sever, T.; Feizpour, D.; Podgornik, B. Impact of Steel Type, Composition and Heat Treatment Parameters on Effectiveness of Deep Cryogenic Treatment. *J. Mater. Res. Technol.* **2021**, *14*, 1007–1020. [[CrossRef](#)]
24. Pellizzari, M. Influence of Deep Cryogenic Treatment on the Properties of Conventional and PM High Speed Steels. *Metall. Ital.* **2008**, *100*, 17–22.
25. Jovičević-Klug, P.; Lipovšek, N.; Jovičević-Klug, M.; Podgornik, B. Optimized Preparation of Deep Cryogenic Treated Steel and Al-Alloy Samples for Optimal Microstructure Imaging Results. *Mater. Today Commun.* **2021**, *27*, 102211. [[CrossRef](#)]
26. Toraya, H. A New Method for Quantitative Phase Analysis Using X-Ray Powder Diffraction: Direct Derivation of Weight Fractions from Observed Integrated Intensities and Chemical Compositions of Individual Phases. *J. Appl. Crystallogr.* **2016**, *49*, 1508–1516. [[CrossRef](#)]
27. Oppenkowski, A.; Weber, S.; Theisen, W. Evaluation of Factors Influencing Deep Cryogenic Treatment That Affect the Properties of Tool Steels. *J. Mater. Processing Technol.* **2010**, *210*, 1949–1955. [[CrossRef](#)]
28. Tyshchenko, A.I.; Theisen, W.; Oppenkowski, A.; Siebert, S.; Razumov, O.N.; Skoblik, A.P.; Sirosh, V.A.; Petrov, Y.N.; Gavriljuk, V.G. Low-Temperature Martensitic Transformation and Deep Cryogenic Treatment of a Tool Steel. *Mater. Sci. Eng. A* **2010**, *527*, 7027–7039. [[CrossRef](#)]

29. Jovičević-Klug, P.; Jenko, M.; Jovičević-Klug, M.; Šetina Batič, B.; Kovač, J.; Podgornik, B. Effect of Deep Cryogenic Treatment on Surface Chemistry and Microstructure of Selected High-Speed Steels. *Appl. Surf. Sci.* **2021**, *548*, 1–11. [[CrossRef](#)]
30. Zhirafar, S.; Rezaeian, A.; Pugh, M. Effect of Cryogenic Treatment on the Mechanical Properties of 4340 Steel. *J. Mater. Processing Technol.* **2007**, *186*, 298–303. [[CrossRef](#)]
31. Jurči, P.; Bartkowska, A.; Hudáková, M.; Dománková, M.; Čaplovičová, M.; Bartkowski, D. Effect of Sub-Zero Treatments and Tempering on Corrosion Behaviour of Vanadis 6 Tool Steel. *Materials* **2021**, *14*, 3759. [[CrossRef](#)]
32. Li, B.; Li, C.; Wang, Y.; Jin, X. Effect of Cryogenic Treatment on Microstructure and Wear Resistance of Carburized 20CrNi2MoV Steel. *Metals* **2018**, *8*, 808. [[CrossRef](#)]
33. Yan, Y.; Luo, Z.; Liu, K.; Zhang, C.; Wang, M.; Wang, X. Effect of Cryogenic Treatment on the Microstructure and Wear Resistance of 17Cr2Ni2MoVNb Carburizing Gear Steel. *Coatings* **2022**, *12*, 281. [[CrossRef](#)]
34. Li, H.; Tong, W.; Cui, J.; Zhang, H.; Chen, L.; Zuo, L. The Influence of Deep Cryogenic Treatment on the Properties of High-Vanadium Alloy Steel. *Mater. Sci. Eng. A* **2016**, *662*, 356–362. [[CrossRef](#)]